

barriers¹⁰ of internal rotors. Where values of $S^\circ(3)$ were lacking, they were estimated by incremental or group additivity methods.⁶ Conversion of ΔS_{ab}° to concentration units gives $\Delta S_{ab}^{\circ,c}$. The results of these calculations are tabulated in the microfilm edition.

Estimation of ΔS_b^\ddagger . ΔS_b^\ddagger was estimated by summing the changes in rotational¹⁰ and vibrational¹⁴ entropy

(10) Both molecular dimensions¹¹ and A values¹² suggest that, when estimating rotational barriers, a methyl group ought to be a satisfactory model for a nitro group. Accordingly, the saturated alkane, obtained by replacing the nitro group in the nitroalkane 3 by a methyl group, was used as a model for estimating rotational barriers in the nitroalkane 3. For example, propane was used as a model for nitroethane. Then, using the methods of Benson and coworkers,⁵ rotational barriers in the nitroalkyl radical 2 or the transition state T^\ddagger were estimated from the rotational barriers estimated for the nitroalkane 3. Rotational barriers in the saturated alkane model compounds were based on literature data.¹³

(11) G. H. Wagniere, "The Chemistry of the Nitro and Nitroso Group," H. Feuer, Ed., Interscience, New York, N. Y., 1969, Part 1, p 1.

(12) J. A. Hirsch, *Top. Stereochem.*, **1**, 199 (1967).

(13) (a) J. Dale, *Tetrahedron*, **22**, 3373 (1966); (b) J. P. Lowe, *Progr. Phys. Org. Chem.*, **6**, 1 (1968); (c) ref 5d.

(14) (a) Torsional frequencies (ω) of the three electron bonds in the transition state (T^\ddagger) were taken to be one-half the magnitude of those estimated for the structurally identical nitro olefin having a full double bond. Torsional frequencies for the nitro olefin were calculated using the formula $\omega \propto [(M_1 + M_2)/M_1 M_2]^{1/2}$. In all calculations the torsional frequency of the olefin, obtained by replacing the NO_2 group in the nitro olefin by a CH_3 group, was used as the reference frequency.^{5d} Other vibrational frequencies were taken from the following references: (b) N. B. Coltrup, "Introduction to Infrared and Raman Spectroscopy," Academic Press, New York, N. Y., 1964; (c) T. Shimanouchi, *Nat. Stand. Ref. Data Ser., Nat. Bur. Stand.*, No. 6 (1967); (d) N. L. Alpert, W. E. Keiser, and H. A. Szymanski, "IR; Theory and Practice of Infrared Spectroscopy," Plenum Press, New York, N. Y., 1970; (e) ref 5d.

produced in the nitroalkyl radical, I, upon passage to the transition state, T^\ddagger . Equation A7 expresses this summation.

$$\begin{aligned} \Delta S_b^\ddagger = & S^\circ[(C-\text{NO}_2)_{rc} + (C-C)_s]^{1300} + \\ & (C-C-\text{NO}_2)_b^{185} + 2(\text{NO}_2)_{le\text{ rock}}^{170} + (C(\uparrow-\text{NO}_2) + \\ & (C-C)_t] - S^\circ[(C-\text{NO}_2)_s]^{825} + (C-C)_s^{1000} + \\ & (C-C-\text{NO}_2)_b^{370} + 2(\text{NO}_2)_{2e\text{ rock}}^{500} + (C(\uparrow-\text{NO}_2) + \\ & (C(\uparrow-C))] + R \ln \{ \sigma_{(2)} / \sigma_{(T^\ddagger)} \} \quad (\text{A7}) \end{aligned}$$

Equation A7 was formulated using the methods and terminology of Benson and O'Neal.^{5d} In formulating eq A7 all entropy terms of magnitude less than 0.1 gibbs mol^{-1} were neglected. The values of ΔS_b^\ddagger computed using eq A7 are listed in the microfilm edition.

Supplementary Materials Available. Two tables will appear following these pages in the microfilm edition of this volume of the journal. The first tabulates our experimental rate constants and the conditions of their measurement. The second summarizes the thermochemical quantities used in or calculated by the thermochemical methods described in the Appendix. Photocopies of the supplementary material from this paper only or microfiche (105 × 148 nm, 24× reduction, negatives) containing all of the supplementary material for papers in this issue may be obtained from the Journals Department, American Chemical Society, 1155 16th St., N.W., Washington, D. C. 20036. Remit check or money order for \$3.00 for photocopy or \$2.00 for microfiche, referring to code number JACS-74-6549.

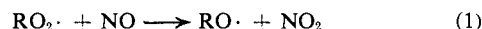
A Long Path Infrared Spectroscopic Study of the Reaction of Methylperoxy Free Radicals with Nitric Oxide

C. T. Pate, B. J. Finlayson, and J. N. Pitts, Jr.*

Department of Chemistry and Statewide Air Pollution Research Center, University of California, Riverside, California 92502. Received April 22, 1974

Abstract: The reaction of NO with CH_3O_2 radicals generated in the photooxidation of $\text{CH}_3\text{N}_2\text{CH}_3$ at $\lambda > 320$ nm was investigated at $23 \pm 2^\circ$ using long path infrared and gas chromatographic techniques. Reaction conditions were: $\text{CH}_3\text{N}_2\text{CH}_3$, 33–369 mTorr; O_2 , 2200–5320 mTorr; and NO, 25–76 mTorr, at a total pressure of 760 Torr (He or N_2). At short photolysis times, CH_3ONO and NO_2 were both identified as products with quantum yields of 1.7 ± 0.2 and 1.9 ± 0.3 , respectively. HCHO was qualitatively identified in several runs by the chromotropic acid test. At longer reaction times, methyl nitrate also accumulated. These results suggest that the reaction $\text{CH}_3\text{O}_2 + \text{NO} \rightarrow \text{CH}_3\text{O} + \text{NO}_2$ (7) is the only path for the reaction of methylperoxy radicals with nitric oxide under these conditions. CH_3O is then removed by the reactions: $\text{CH}_3\text{O} + \text{NO}_2 \rightarrow \text{CH}_3\text{ONO}_2$ (9a), $\text{CH}_3\text{O} + \text{NO}_2 \rightarrow \text{HCHO} + \text{HONO}$ (9b), $\text{CH}_3\text{O} + \text{NO} \rightarrow \text{CH}_3\text{ONO}$ (8a), and $\text{CH}_3\text{O} + \text{NO} \rightarrow \text{HCHO} + \text{HNO}$ (8b).

The reaction of alkylperoxy radicals with nitric oxide is generally assumed^{1–3} to proceed by the oxidation of nitric oxide to nitrogen dioxide with formation of an alkoxy radical



(1) H. Niki, E. E. Daby, and B. Weinstock, *Advan. Chem. Ser.*, No. 113, 16 (1971).

(2) A. P. Altshuller and J. J. Bufalini, *Photochem. Photobiol.*, **4**, 97 (1965).

(3) T. A. Hecht and J. A. Seinfeld, *Environ. Sci. Technol.*, **6**, 47 (1972).

Reaction 1 is believed to be an important route for oxidizing NO to NO_2 in photochemical smog. In addition, the alkoxy radical, $\text{RO} \cdot$, may react further in the atmosphere to produce $\text{HO}_2 \cdot$ ⁴ which also converts NO to NO_2 . However, a mass spectrometric study⁵ in-

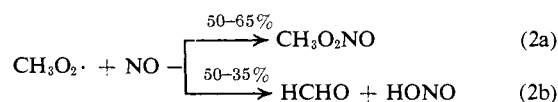
(4) J. Heicklen, K. Westberg, and N. Cohen, Center for Air Environmental Studies Report No. 115-69, The Pennsylvania State University, 1969.

(5) C. W. Spicer, A. Villa, H. A. Wiebe, and J. Heicklen, *J. Amer. Chem. Soc.*, **95**, 13 (1973).

Table I. Columns Used in Gas Chromatographic Analysis of the Products of the Photooxidation of Azomethane in the Presence of NO at Room Temperature

Column designation	Column description	Carrier gas flow rate, ml/min	Column temp, °C	Compd identified	Model and detector
A	3 m × 3 mm 10% Carbowax 600 on 100–120 acid washed firebrick	25	23	CH ₃ ONO, CH ₃ ONO ₂	Varian Aerograph Hy-Fy 600, electron capture detector
B	3 m × 3 mm 10% Carbowax 600 on 100–120 acid washed firebrick	50	50	CH ₃ ONO, CH ₃ ONO ₂ , CH ₃ NO ₂	Varian Aerograph 1400 with flame ionization detector
C	3 m × 3 mm 10% Carbowax 600 on 100–120 acid washed firebrick	50	23	CH ₃ ONO, CH ₃ ONO ₂	Finnigan Model 3100 combined gas chromatograph mass spectrometer
D	3 m × 3 mm 20% XF 1150 cyanosilicone on 80–100 HMDS treated Chromosorb	23	23	CH ₃ ONO	Varian Aerograph 1400 with flame ionization detector
E	6 m × 6 mm Linde molecular sieve, 13X	30	0	N ₂ , O ₂	Perkin-Elmer 900, thermal conductivity detector

icated that reaction 1 with R = CH₃ does not occur as written but rather proceeds as follows.



Secondary reactions of the HCHO and of the CH₃O₂NO adduct with O₂ were postulated to form formic acid and methyl nitrate, the observed products.⁵ More recent studies⁶ suggest that the reaction of NO with CH₃O₂· occurs *via* reaction 1 approximately 79 ± 8% of the time.

We report here a reinvestigation of this important reaction by long path infrared (lpir) spectroscopy and gas chromatography (gc), using millitorr reactant concentrations. The results of this study confirm that methylperoxy radicals do react with nitric oxide as shown in reaction 1; no evidence for the existence of alternate reaction paths was found.

Experimental Section

Chemicals. Azomethane (Merck Sharp and Dohme) was degassed at liquid nitrogen temperature and then passed through Ascarite (Arthur H. Thomas, Co.) to remove traces of carbon dioxide. Nitric oxide (Matheson, ≥99.0%) was passed through Linde molecular sieve 13X to remove any NO₂ and water present. NO₂ (Matheson, ≥99.0%) was distilled over oxygen. The O₂ (Liquid Carbonic, ≥99.95%), N₂ (Matheson, ≥99.995%), and He (Liquid Carbonic, ≥99.995%) were used as received.

Authentic samples of methyl nitrite⁷ and methyl nitrate⁸ were prepared by standard procedures. The methyl nitrite was purified by passage through sodium bicarbonate and Ascarite. The methyl nitrate was purified by gc.

Apparatus. Irradiations were carried out in an FEP Teflon coated cylindrical vessel (25-cm diameter, 95-cm length) which housed the White cell optics of the 40-m path length Perkin-Elmer Model 621 infrared spectrometer. The cell was evacuated to 6.0 × 10⁻⁴ Torr between runs. Unfiltered light from a medium pressure 1200-W mercury arc (Hanovia Model 3A-44V) entered the sample tank through six 7.5 × 7.5 cm ports of 6 mm thick window plate which transmitted light of λ > 320 nm. Hence the 366 nm mercury line was the primary photolytic wavelength.⁹ For several runs the light intensity was reduced with wire screens in order to determine its effect on the reaction.

(6) R. Simonaitis and J. Hecklen, personal communication, 1974.

(7) W. H. Hartung and F. Crossley, "Organic Syntheses," Collect. Vol. II, Wiley, New York, N. Y., 1943, p 363.

(8) A. P. Black and F. H. Babers, ref 7, p 412.

(9) J. G. Calvert and J. N. Pitts, Jr., "Photochemistry," Wiley, New York, N. Y., 1966, and references therein.

Procedures. Reaction mixtures were prepared by expansion from a calibrated volume of known pressures (MKS Baratron Type 90, 0–10 Torr pressure gauge) of the reactants into the reaction chamber of the lpir followed by pressurizing to 760 Torr with He or N₂. Initial concentrations were: CH₃N₂CH₃, 33–369 mTorr; NO, 25–76 mTorr; O₂, 2200–5320 mTorr. These reactant concentrations were chosen to minimize the thermal oxidation of NO to NO₂^{10,11} and the reaction of CH₃· with NO.^{12,13} Dark runs confirmed that the thermal conversion of NO to NO₂ was negligible during the short duration of these experiments (~15 min).

The extinction coefficients for CH₃N₂CH₃, CH₃ONO₂, and NO₂ were determined from Beer's law studies of measured millitorr concentrations of each of these compounds in 760 Torr of He or N₂. During an experiment, methyl nitrite (CH₃ONO) was determined from its absorbance at 800 cm⁻¹. Nitrogen dioxide (NO₂) was determined from the total absorbance at 1600 cm⁻¹ by subtracting out that due to CH₃ONO. Methyl nitrate (CH₃ONO₂) was measured from its absorbance at 1300 cm⁻¹.

In some runs, methyl nitrite, methyl nitrate, and other products were also monitored by gc or combined gas chromatography–mass spectrometry (gc–ms). Table I lists the columns, detectors, and operating conditions used.

A search for HCHO was also carried out by flushing the contents of the cell through two traps in series containing distilled water and subsequently identifying HCHO by the chromotropic acid test.¹⁴

Actinometry was done by photolyzing measured concentrations of azomethane in 760 Torr of He and following the rate of nitrogen formation using column E of Table I. Since the quantum yield for N₂ formation from azomethane is 1.0,¹⁵ the rate of its formation is also the rate of light absorption by azomethane, I_a. As a check, N₂ was also monitored during one experiment with NO and O₂ present and its rate of formation was shown to agree with that determined in actinometry runs.

Results

Figures 1a and 1b show typical infrared spectra of the individual reactants and products. These spectra agree well with those reported in the literature.^{16–18} The

(10) J. Hecklen and N. Cohen, *Advan. Photochem.*, **5**, 157 (1968).

(11) D. H. Stedman and H. Niki, *Environ. Sci. Technol.*, **7**, 735 (1973).

(12) N. Basco, D. G. L. James, and R. D. Suart, *Int. J. Chem. Kinet.*, **2**, 215 (1970).

(13) N. Basco, D. G. L. James, and F. C. James, *Int. J. Chem. Kinet.*, **4**, 129 (1972).

(14) P. W. West and B. Sen, *Z. Anal. Chem.*, **153**, 12 (1956), and references therein.

(15) M. H. Jones and E. W. R. Steacie, *J. Chem. Phys.*, **21**, 1018 (1953).

(16) R. H. Pierson, A. N. Fletcher, and E. Gantz, *Anal. Chem.*, **28**, 1218 (1956).

(17) P. Klabeo, D. Jones, and E. R. Lippincott, *Spectrochim. Acta, Part A*, **23**, 2957 (1967).

(18) E. R. Stephens and M. A. Price, ir spectrum of CH₃ONO₂, personal communication, 1974.

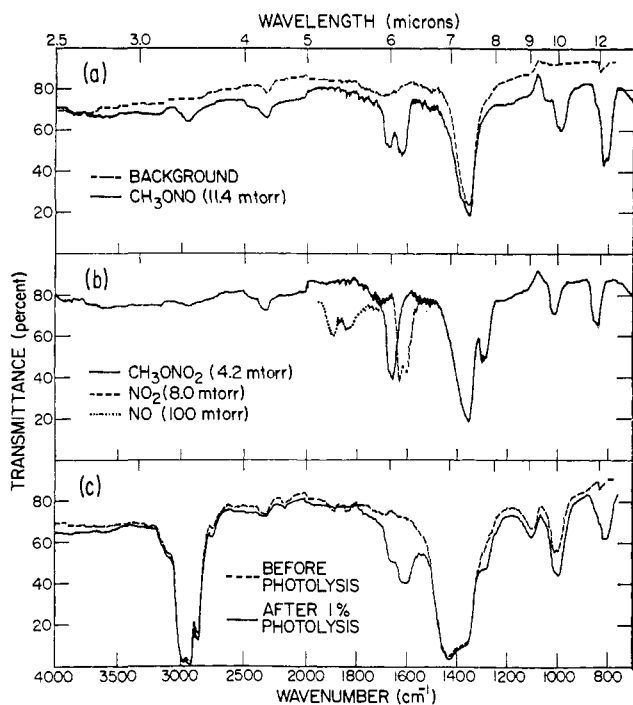


Figure 1. (a) Infrared spectrum of the empty cell and of 11.4 mTorr of CH₃ONO. (b) Infrared spectrum of 100 mTorr of NO, 8.0 mTorr of NO₂, 4.2 mTorr of CH₃ONO₂. (c) Infrared spectrum before and after 1% photolysis of 340 mTorr of azomethane, 39 mTorr of NO, and 3130 mTorr of O₂.

limits of detection of the products and the relevant extinction coefficients are given in Table II. Figure 1c

Table II. Infrared Extinction Coefficients^a and Limits of Detection of Some Reactants and Products in the Photooxidation of Azomethane in the Presence of NO at Room Temperature

Compd	Wave number, cm ⁻¹	Extinction coefficient, mTorr ⁻¹ m ⁻¹	Detection limit, mTorr
CH ₃ N ₂ CH ₃	1000	1.46×10^{-5}	
CH ₃ ONO	800	5.63×10^{-4}	0.5
	1600	3.03×10^{-4}	
NO ₂	1600	9.15×10^{-4}	0.6
CH ₃ ONO ₂	1300	9.58×10^{-4}	0.5

^a To base 10.

gives the infrared spectrum of a typical reactant mixture before and after photolysis to 1% conversion of azomethane. It is seen that the only detectable products are NO₂, CH₃ONO, and small amounts of CH₃ONO₂. Extensive analysis by gc (Table I) confirmed the presence of CH₃ONO and CH₃ONO₂ and revealed traces of CH₃NO₂ and one other unidentified product. Small amounts of HCHO were also detected by the chromotropic acid test.¹⁴ The observation of these products is in agreement with an earlier lpir study¹⁹ of this system, as well as with the more recent gc studies⁶ of this reaction.

Figure 2 shows a typical plot of product formation and NO loss with time. Both CH₃ONO and NO₂ grow linearly during the initial stages of the reaction when CH₃ONO₂ formation is negligible. At longer reaction

(19) P. L. Hanst and J. G. Calvert, *J. Phys. Chem.*, **63**, 2071 (1959).

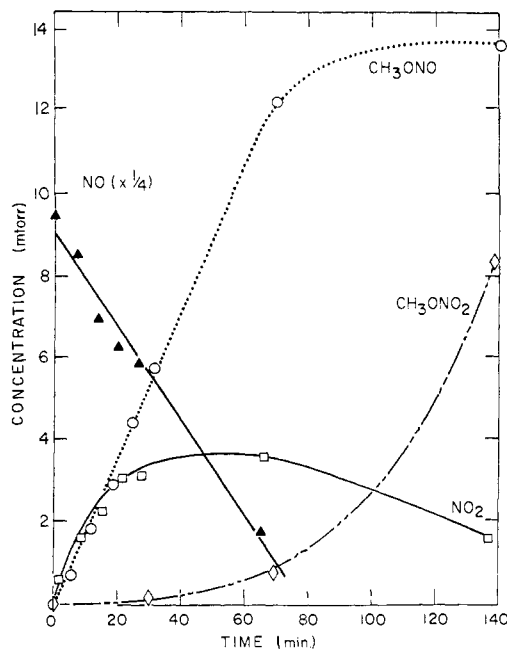


Figure 2. Typical time dependence of CH₃ONO, CH₃ONO₂, NO₂, and NO in the photooxidation of azomethane in the presence of NO. Initial conditions: azomethane 132 mTorr; O₂ 2830 mTorr; NO 38 mTorr.

times the NO₂ concentration levels off and the CH₃ONO₂ begins to increase nonlinearly. Finally, at low NO concentrations, the rate of CH₃ONO formation falls, while that of CH₃ONO₂ increases substantially.

The low extinction coefficient for NO at 1900 cm⁻¹ (4×10^{-5} mTorr⁻¹ m⁻¹) precludes its accurate measurement by infrared at the low concentrations used in these experiments. For example, the point at 65 min in Figure 2 corresponds to the limit of detection of NO in this system. Hence the NO data even at short reaction times are only accurate to about $\pm 15\%$.

The quantum yields of CH₃ONO and NO₂ were calculated as the ratio of their initial rates of formation to the rate of azomethane loss. Because both NO₂ and CH₃ONO absorb light of $\lambda > 320$ nm,^{9,20,21} their quantum yields were calculated under conditions such that their loss by photolysis was small. Since the extinction coefficients for NO₂ and CH₃ONO at 366 nm are 1.5×10^2 and 48 l. mol⁻¹ cm⁻¹, respectively, compared to 31. mol⁻¹ cm⁻¹ for CH₃N₂CH₃,⁹ all quantum yields were determined under conditions such that $[\text{CH}_3\text{N}_2\text{CH}_3]/[\text{NO}_2] > 50$ and $[\text{CH}_3\text{N}_2\text{CH}_3]/[\text{CH}_3\text{ONO}] > 15$.

Table III gives, for a series of runs of varying initial reactant concentrations and light intensity: (1) the initial rates of product formation as a ratio to the azomethane concentration and (2) the corresponding quantum yields. The NO₂ quantum yield is 1.9 ± 0.3 while that for CH₃ONO is 1.7 ± 0.2 where the specified errors represent one standard deviation. An upper limit for the quantum yield of CH₃ONO₂ is 0.01 from its initial rate of formation. Typically, CH₃ONO₂ was not detected by gc (detection limit $\sim 4 \times 10^{-3}$ mTorr) in the first 3 min of photolysis.

(20) G. R. McMillan, J. Kumari, and D. L. Snyder, "Chemical Reactions in Urban Atmospheres," C. S. Tuesday, Ed., Elsevier, Amsterdam, 1969, pp 35-44.

(21) I. T. N. Jones and K. D. Bayes, *J. Chem. Phys.*, **59**, 4836 (1973), and references therein.

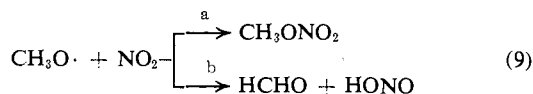
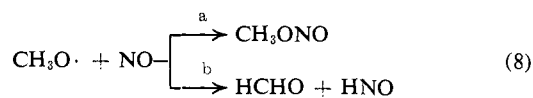
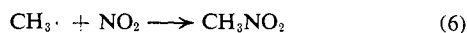
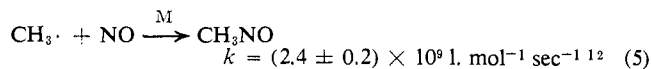
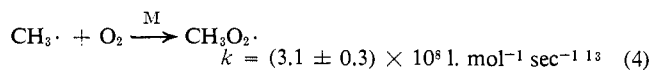
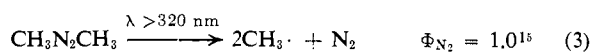
Table III. Reactant Concentrations, Rates of Product Formation, and Quantum Yields for the Photooxidation of Azomethane in the Presence of NO at Room Temperature

Initial reactant concn, ^a mTorr			$R_{\text{CH}_3\text{ONO}}^b \times 10^3 /$	$\Phi_{\text{CH}_3\text{ONO}}$	$R_{\text{NO}_2}^b \times 10^3 /$	Φ_{NO_2}
$[\text{CH}_3\text{N}_2\text{CH}_3]_0$	$[\text{NO}]_0$	$[\text{O}_2]_0$	$[\text{CH}_3\text{N}_2\text{CH}_3]_0, \text{min}^{-1}$		$[\text{CH}_3\text{N}_2\text{CH}_3]_0, \text{min}^{-1}$	
			$I_a = (7.0 \pm 0.7) \times 10^{-4} \text{min}^{-1 c}$			
369	37	3040	0.99	1.4	1.4	2.0
340	39	3130	1.1	1.5	1.2	1.7
322	40	3340	1.2	1.7	1.1	1.5
289	39	3040	1.1	1.6	1.3	1.8
253	36	3040	1.2	1.8	1.6	2.3
217	30	3040	1.1	1.6	1.4	1.9
204	37	3040	1.2	1.7	1.6	2.3
149	36	3040	1.2	1.7	1.3	1.8
132	38	2830	1.3	1.9	1.4	2.0
97	36	3040	1.3	1.9	1.3	1.9
33	25	3040	1.5	2.2	1.8	2.6
241	67	3040	1.3	1.8	1.2	1.7
268	52	3040	1.2	1.7	1.1	1.6
239	44	3040	1.2	1.7	1.5	2.1
270	30	3040	1.1	1.6	1.3	1.9
336	37	5320	1.1	1.6	1.3	1.9
250	37	3800	1.1	1.6	NA ^d	NA ^d
295	39	2280	0.91	1.3	1.1	1.6
275	38	2200	1.1	1.5	1.2	1.7
163	57	3040	1.1	1.6	1.2	1.7
153	76	3040	1.3	1.8	1.5	2.1
172	56	3040	1.3	1.9	1.3	1.9
			1.2 ± 0.1		1.3 ± 0.2	
			$I_a = (1.3 \pm 0.1) \times 10^{-4} \text{min}^{-1 c}$			
349	41	3040	0.19	1.5	0.28	2.2
314	41	3040	0.19	1.5	0.22	1.7
			$I_a = (0.88 \pm 0.09) \times 10^{-4} \text{min}^{-1 c}$			
239	40	3040	0.19	2.2	0.18	2.1
			1.7 ± 0.2		1.9 ± 0.3	

^a 1 mTorr = 1.3 ppm (parts per million). ^b $R_{\text{CH}_3\text{ONO}}$ and R_{NO_2} are rates of formation of methyl nitrite and nitrogen dioxide, respectively. ^c I_a is the rate of light absorption by $\text{CH}_3\text{N}_2\text{CH}_3$. ^d NA = not available.

Discussion

The following reactions describe the photooxidation of azomethane in the presence of the nitric oxide under these conditions.



Under these experimental conditions, removal of $\text{CH}_3\cdot$ by reaction with $\text{NO}^{12,13}$ will occur $\lesssim 10\%$ of the time, particularly since the NO concentration is decreasing during the reaction. At low azomethane conversions ($\sim 1\%$) the contribution of reaction 6 to the removal of $\text{CH}_3\cdot$ radicals is also small, although it does account for the trace quantities of CH_3NO_2 observed by gc.

The reaction (reaction 8) of methoxy radicals with NO can occur either by combination (step a) or by abstraction (step b) with $k_{8b}/k_8 = 0.143$.²²⁻²⁵ Similarly, reaction 9, which is minimal at short reaction times, can also occur by combination or abstraction with $k_{9b}/k_9 = 0.08$.²³ Estimates of the rate constant ratio k_8/k_9 range from 1.2²³ to 2.9.^{26,27} Hence reaction 9 will become competitive with reaction 8 at longer reaction times when the NO concentration approaches that of NO_2 . Reaction 10 is too slow^{23,25,28} ($k_{10} = 1.6 \times 10^3 \text{ l. mol}^{-1} \text{ sec}^{-1}$) to be significant under these conditions.

Our experimental results are consistent with the above scheme in that (1) the major products at short photolysis times are CH_3ONO and NO_2 , (2) NO_2 accumulates linearly with time until its removal by both reaction 9 and photolysis becomes competitive with its rate of formation, and (3) small amounts of HCHO and CH_3NO_2 are observed. At longer reaction times, reaction 9 becomes competitive with reaction 8 and hence the CH_3ONO_2 concentration increases and NO_2 decreases. Simultaneously, the rate of CH_3ONO formation falls. HCHO was not detected by ir since its detection limit in

(22) H. A. Wiebe and J. Hecklen, *J. Amer. Chem. Soc.*, **95**, 1 (1973).

(23) H. A. Wiebe, A. Villa, T. M. Hellman, and J. Hecklen, *J. Amer. Chem. Soc.*, **95**, 7 (1973).

(24) G. E. McGraw and H. S. Johnston, *Int. J. Chem. Kinet.*, **1**, 89 (1969).

(25) W. Glasson, Abstracts, 167th National Meeting of the American Chemical Society, Los Angeles, Calif., March 31–April 5, 1974, Phys. No. 41.

(26) G. Baker and R. Shaw, *J. Chem. Soc.*, 6965 (1965).

(27) P. Gray, R. Shaw, and J. C. J. Thynne, *Progr. React. Kinet.*, **4**, 63 (1967).

(28) J. Hecklen, *Advan. Chem. Ser.*, No. 76, 23 (1968).

this system is ~ 3 mTorr and the maximum yield of HCHO from reactions 8b and 9b in any of these runs was 2.3 mTorr. Under these conditions, loss of HCHO by photolysis is negligible.⁹

Estimates of the rates of reaction of HNO with itself and with O_2 ^{28, 29} indicate that these rates are sufficiently slow that HNO should accumulate in this system. While the ir extinction coefficient for HNO is unknown, it is not surprising that the low yield is below our detection limit. The same is true of the small yields of CH_3NO anticipated from reaction 5. At these low conversions, HONO is also expected to be undetected.³⁰

Both our experimental results and the kinetic data available in the literature suggest that for the purposes of kinetic analysis, at short photolysis times where the loss of NO_2 is negligible, reactions 5, 6, 9, and 10 may be neglected. Using a simplified scheme consisting of the remaining reactions 3, 4, 7, and 8, one can derive the following relations.

$$R_{NO_2} = d[NO_2]/dt = 2.0I_a[CH_3N_2CH_3]_0 \quad (I)$$

$$R_{CH_3ONO} = d[CH_3ONO]/dt = 1.71I_a[CH_3N_2CH_3]_0 \quad (II)$$

I_a is the rate of light absorption by azomethane in reciprocal minutes and $[CH_3N_2CH_3]_0$ is the initial azomethane concentration. Hence $R_{NO_2}/[CH_3N_2CH_3]_0$ and $R_{CH_3ONO}/[CH_3N_2CH_3]_0$ should be independent of initial reactant concentrations, as found (Table III). From the average values of these ratios, $I_a = 6.5 \pm 1.0 \times 10^{-4} \text{ min}^{-1}$ from NO_2 formation and $I_a = 7.0 \pm 0.7 \times 10^{-4} \text{ min}^{-1}$ from CH_3ONO formation, within 7% of the value $7.0 \pm 0.7 \times 10^{-4} \text{ min}^{-1}$ determined in separate actinometry experiments. This scheme also predicts quantum yields of 2.0 and 1.7 for NO_2 and CH_3ONO , respectively, in excellent agreement with the results given in Table III.

The carbon and nitrogen mass balances in the initial stages of the reaction are reasonably good. For example, in Figure 2, 1.9 ± 0.20 mTorr of NO_2 and 1.8 ± 0.09 mTorr of CH_3ONO have been produced at 10 min while 4.7 ± 0.7 mTorr of NO and 0.92 ± 0.1 mTorr of $CH_3N_2CH_3$ have reacted. According to the above mechanism, 3.7 ± 0.6 mTorr of NO is predicted to react during this time interval. Since $k_{8a}/k_8 = 0.86$, the carbon and nitrogen balances are 110 ± 20 and $85 \pm 30\%$, respectively. The particularly large uncertainty in the nitrogen balance is due to the inaccuracies in

(29) K. L. Demerjian, J. A. Kerr, and J. G. Calvert, *Advan. Environ. Sci. Technol.*, **4**, 1 (1973).

(30) L. H. Jones, R. M. Badger, and G. E. Moore, *J. Chem. Phys.*, **19**, 1599 (1951).

measuring NO by infrared spectroscopy as discussed above, which precludes accurate mass balance computations in the present system. At long reaction times, however, it appears that the nitrogen balance may be somewhat poorer. For example, at 140 min the percentages of carbon and nitrogen accounted for in the observed products are 103 ± 20 and $71 \pm 30\%$, respectively. This is likely due to secondary reactions producing nitrogen compounds which are not easily detected by Ipir and gc or which may be adsorbed on the walls. Since this study was concerned only with the mechanism at short reaction times where all the carbon and nitrogen could be accounted for, no further investigations of the poor nitrogen balance at longer photolysis times were done.

Our observations of the time dependence of methyl nitrate formation are in agreement with those of earlier investigators⁵ in that it is formed with an "induction period" which depends on the rate of light absorption. This is understandable since according to the above mechanism

$$d[NO]/dt = -4I_a[CH_3N_2CH_3]_0 \quad (III)$$

Higher rates of light absorption correspond to higher rates of NO loss, hence reaction 9 forming CH_3ONO_2 will become competitive with reaction 8 at shorter reaction times. In addition, it appears that with the rate of loss of NO given in eq III, little NO would remain after the induction periods found by these investigators⁵ and hence secondary reactions might well then produce HCOOH. It is puzzling, however, that CH_3ONO was not detected in their studies in the early stages of the reaction, either by mass spectrometry or gas chromatography.⁵

In conclusion, our results confirm that under these experimental conditions, methylperoxy radicals oxidize NO to NO_2 . We find no evidence of alternate modes of reaction occurring between these two species.

Acknowledgment. This project has been financed in part with funds from the Environmental Protection Agency under Grant No. 800649 and partly from NSF Grant GP-38053X. The contents do not necessarily reflect the views and policies of the Environmental Protection Agency, nor does the mention of trade names or commercial products constitute endorsement or recommendation for use. We wish to thank Mr. M. A. Price and Dr. E. R. Stephens for supplying purified samples of methyl nitrate. We are also grateful to Finnigan Corporation, and especially Mr. T. Z. Chu, for the use of a gc-ms during this work.